Wiley
Journal of Applied Ichthyology
Volume 2024, Article ID 6597804, 15 pages
https://doi.org/10.1155/2024/6597804

WILEY

Research Article

Assessment of Sex, Gonad Volume, and Reproductive Maturation Status of the Indian Shad, *Tenualosa ilisha*, Using Ultrasonic Imaging: A Rapid and Non-Invasive Tool

Subrata Dasgupta ,[1] Gouranga Biswas ,[1] Gayatri Tripathi,[2] Mujahidkhan A. Pathan ,[2] Tapas K. Ghoshal,[1] Pratiksha K. Singh,[1] Tanmoy Jana,[1] Paroma Mitra,[1] Srikanta Samanta,[3] Debasis De,[4] Subhendu Adhikari,[5] Ranjan K. Manna,[3] and Amiya K. Sahoo[3]

[1]*ICAR-Central Institute of Fisheries Education, Kolkata Centre, 32-GN Block, Sector-V, Salt Lake City, Kolkata 700091, India*
[2]*ICAR-Central Institute of Fisheries Education, Panch Marg, Off Yari Road, Versova, Andheri (West), Mumbai 400061, India*
[3]*ICAR-Central Inland Fisheries Research Institute, Barrackpore, Kolkata 700120, India*
[4]*ICAR-Central Institute of Brackishwater Aquaculture, Kakdwip Research Centre, South 24 Pargana, Kakdwip, West Bengal 743347, India*
[5]*ICAR-Central Institute of Freshwater Aquaculture, Regional Research Station, Rahara, Kolkata 700118, West Bengal, India*

Correspondence should be addressed to Gouranga Biswas; g.biswas@icar.gov.in

Received 23 December 2023; Revised 3 July 2024; Accepted 30 July 2024

Academic Editor: Mohd Rather

To determine sex and maturity stages accurately without any physical injury and stress, especially for sensitive and high-value fish species, employing a noninvasive ultrasound imaging technique could be a desirable approach. The ultrasound imaging method as a powerful eco-friendly tool was established to determine sex, gonad volume, gonadosomatic index (GSI), and reproductive stages in the Indian shad, hilsa (*Tenualosa ilisha*). About 30 hilsa (15 males and 15 females) of different maturity stages were collected from the river Ganga round the year using gill nets. The ultrasound sonography (USG) was then employed in hilsa to determine the computed GSI. The fresh gonad volume of hilsa was determined using a water displacement method to ascertain actual GSI values. There was no significant difference between the calculated, real, and actual GSIs ($P > 0.05$) in both males and females. The validation of the precise maturity stages of ultrasound images of the gonad by the histological architecture indicated that USG images of the hilsa gonad depicted exact stages of maturity in both sexes except for stages I and II in males. The sex of the fish was accurately ascertained using ovarian ultrasound scanning for all the specimens. The calculated USG-based ovarian volume was positively correlated ($R^2 = 0.97$) with the actual and real ovarian volumes. The noninvasive and reliable ultrasonography technique was found to be an accurate and valid tool to track gender and gonadal development and predict the spawning periodicity in hilsa.

1. Introduction

The yearly gonadal cycle and spawning pattern of fish need precise estimation to understand the reproductive biology [1–5]. To understand the reproductive indices (such as sex ratio, reproductive structure, and spawning periodicity) of a population, fish biologists must ascertain the sex and maturity status of fish. Reproductive indices are valuable for managing and conserving fisheries. Assessing them can be challenging, as it involves sacrificing fish and labour-intensive and time-consuming work (gonadal histology, for example). Consequently, fish biologists searched nonlethal methods to evaluate reproductive indices to avoid sacrificing valuable brood fish. Therefore, to exclude potential detrimental effects on gonads or muscles and consequent mortality, a reliable approach for determining maturity is essential in the efficient broodstock of valuable species. Gender identification and maturity assessment in many fish species have been attempted by employing noninvasive ultrasound technology [6–10]. The Indian shad or hilsa shad (*Tenualosa ilisha*, Hamilton 1822) fishery in South Asia is a lucrative open-access fishery, with Bangladesh's share being 50–60% of the world's hilsa catch [11, 12]. The species is one of the most valuable ones [13, 14] in the Indian subcontinent [15]. Hilsa is an anadromous Clupeid (Figure 1) [12, 16] that breeds during the post-monsoon season in river courses surrounding the Northern Bay of Bengal [15, 17, 18]. Bangladesh and India are two countries that economically use hilsa stocks, but Bangladesh has a higher total production than India [16]. West Bengal, located close to Bangladesh's international border [17] (Figure 2), produces the majority of India's hilsa catch (70–80%), even though it often cannot meet its demand and imports a large quantity of hilsa and related products from Bangladesh [19]. Hilsa fishery provides livelihoods to 2% of the Bangladesh population [15].

In Bangladesh and West Bengal, the hilsa stock has been overexploited for a long time [12, 20]. Overfishing occurs mostly during the spawning, grazing, feeding, and development seasons [21]. India has launched a National Plan of Action for hilsa to restore the health of its hilsa stock and fisheries, and Bangladesh has implemented measures, such as limitations on fishing gear, exclusive closure of certain areas for hilsa fishing, fishing season restrictions, and vessel rules [22]. Bangladesh has also implemented a sustainable management approach for its hilsa stock through a "payment for ecosystem services (PES) scheme" [23].

Captive breeding programmes are widely applied for conserving, reintroducing, and supplementing populations of declining migratory fisheries. Recently, India has made a phenomenal progress in captive rearing of hilsa [24]. Despite this, the captive breeding of hilsa could not be attempted due to lack of understanding on the reproductive biology of pond-reared hilsa. The absence of reliable and ethical techniques for identifying the gender and maturity level of brood fish poses a challenge for intervening in hormonal manipulation of captive maturation in hilsa. Many methods and techniques currently employed for determining sex and maturity are both time-consuming and labour-intensive, causing a threat to the health and reproductive success of fish. These methods often involve collection of blood and oocytes, which can cause stress to mature brood fish, introduce pathogens, and prevent the progress of maturation and ovulation. The stress induced by catheterization and blood sampling can even lead to direct mortalities. Furthermore, these approaches are not always definitive in determining the sex or reproductive status of fish throughout the year, especially outside the spawning season. Ultrasound sonography (USG), a noninvasive technique, is often used to capture images of gonads in fish. Its main applications include determining the gender and monitoring their maturation status. This method offers several advantages, such as availability of portable equipment and short examination duration with minimal stress.

Several studies have employed ultrasonography to examine gender and maturity in varieties of fish species. Reimers et al. [25, 26] assessed sex and maturity in salmon

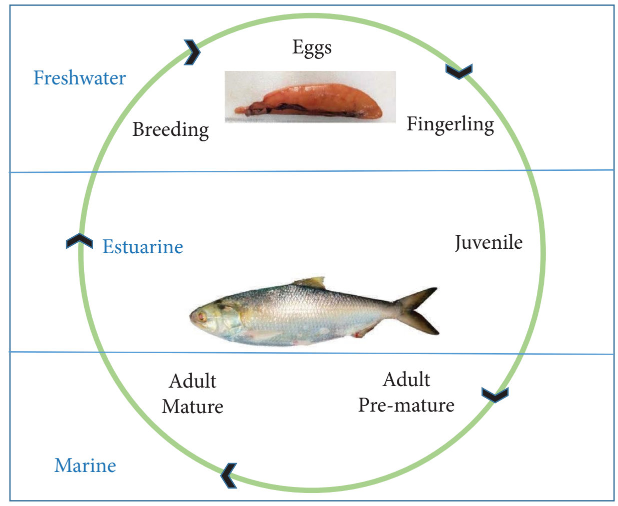

Figure 1: Life cycle of hilsa with migration pattern and different phases from marine to freshwater ecosystems.

based on USG images. Bonar et al. [27] captured ultrasound images to determine the sex and maturity of Pacific herring without causing any harm. Martin-Robichaud and Rommens [28] used USG to evaluate the sex and ovarian maturation of halibut and flounder. Jennings et al. [29] measured ovary volume and estimated fecundity in striped bass, *Morone saxatilis*. Bryan et al. [7] estimated gonad volume, fecundity, and reproductive stage in shovelnose sturgeon using sonography. McEvoy et al. [30] identified the gender of cod, *Gadus morhua* based on ultrasonographic appearance. Whittamore et al. [31] validated USG as an accurate method for assessing internal reproductive structures in oviparous elasmobranchs. Masoudifard et al. [32] demonstrated that ultrasound imaging is a quick, valid, and noninvasive method for determining the sex of a 3-year-old cultured Beluga sturgeon, *Huso huso* Petochi et al. [33] examined the sex and stage of gonad maturity in 6-year-old sturgeon hybrids using ultrasonography. Guitreau et al. [34] worked on developing rapid, straightforward, and minimally stressful procedures for ultrasound imaging of ovaries in channel catfish, *Ictalurus punctatus*. Hliwa et al. [35] assessed the morphology of gonadal structure in sex-reversed rainbow trout females using ultrasound. Bureau du Colombier et al. [36] demonstrated the noninvasive ultrasonography for sex determination and maturation monitoring in silver eels.

Studies on ultrasonography in fish vary in approaches including handling methods, type of equipment, instrument settings, and image analysis. Such variations in the operational procedures are influenced by the specific objectives of study and the species being investigated. The accuracy of USG-based sex identification relies on size, sex, and maturation status of fish. Previous studies demonstrated that gonad volume, gonadosomatic index (GSI), and reproductive stage of fish can be assessed using ultrasonographic techniques. However, there is no existing documentation on the use of ultrasonography for determining sex and assessing gonadal maturity in hilsa. We

Figure 2: Maps illustrating the locations of sampling sites along the Ganga River system in West Bengal, India's Hooghly-Bhagirathi stretch. Live hilsa were collected from the sites indicated on the map.

developed and cross-validated USG procedures using the wild hilsa since captive broodstock of hilsa was scarce. The study aimed to determine the maturity markers (GSI and ovarian volume) to establish a rapid and noninvasive USG method for determining sex and reproductive status in the wild *T. ilisha* for the first time. This technique could be applied to evaluate the reproductive indices of captive and wild hilsa populations in a nonlethal way for developing effective policies to conserve the precious species *in situ* and *ex situ*. Moreover, this technique could be applied to determine better intervention for gonadal maturation and spawning in captive-reared hilsa.

2. Materials and Methods

2.1. Sampling Sites and Sample Collection. During 2022-2023, live fish samples were collected along the Hooghly-Bhagirathi River of the Ganga River System. A total of 30 hilsa (15 males and 15 females) were collected from the Hooghly-Bhagirathi stretch of the Ganga River System at specific sampling locations at Diamond Harbour (Lat. 22°39′18.5364″N and Long. 88°20′25.9908″E), Bally (Lat. 22°25′48.00″N and Long. 87°52′12.00″E), Godakhali (Lat. 22°10′10″N and Long. 88°46′45″E), and Kolaghat (Lat. 22°11′34.91″N and Long. 88°11′4.78″E) (Figure 2) during September 2022 through September 2023. Live fish were caught using drift gill nets (mesh size >65 mm) operated on the motorized fishing boats. The mean total length and body weight of female hilsa were 309.2 ± 53.68 mm and 361.33 ± 153.20 g, respectively. On the other hand, the male hilsa fish had a mean total length and body weight of 260.59 ± 30.98 mm and 252.33 ± 65.32 g, respectively. After collection, the fish were kept in 30-L circular tanks filled with river water maintaining a temperature between 26 and 28°C under natural light and constant aeration during a short acclimation before anesthetization. Females were generally larger than males and exhibited broader body girth than males. The males had pronounced roughness on the dorsal surface, while the females' pectoral fins were smooth during the onset of maturation stages. The urogenital opening of a mature female had a flat appearance, whereas in a mature male, it appeared narrower. During the breeding season, males had elongated abdomens and would release milt when gentle pressure was applied to the ventrolateral sides of the abdomen near the vent. In contrast, females had bulgy abdomens, and ova would spontaneously ooze out when gentle pressure was applied. The identification of sex and determination of gonad morphometrics in 15 males and 15 females were conducted by ultrasound scanning of the body cavity using an ultrasonic device (Aeroscan CD10 Pro/Plus, Konica Minolta Healthcare India Pvt. Ltd., Mumbai). The accuracy of ultrasonic assessment of sex and gonad morphometrics was further confirmed through histology and direct measurement of the gonads of all fish scanned by USG ($n = 15$ females and 15 males). Furthermore, the absolute fecundity of all 15 females was determined using the gravimetric method.

2.2. Anesthesia Procedure. Before scanning, the fish were shifted to tanks filled with river water containing 100–120 mg/L (data unpublished) of MS222 (Sigma, USA). Subsequently, they were collected using a hand net, weighed and recorded for their body length before performing ultrasonography. The fish were handled carefully, wrapped in wet towels, and placed on a tray. After a sonographic examination of the gonads, all the fish were ventrally dissected, and both the left and right lobes of gonad were individually collected and measured for length and weight. Gonad volume was measured following the standard gravimetric method. Then, subsamples from each gonad were kept for histological examination and fecundity determination.

2.3. Sonographic Examinations. The anesthetized *T. ilisha* was placed on a wet towel before sonographic examination [37]. Fish were held in a dorsal recumbent position, or ventral side up. Using an ultrasonic probe perpendicular to the body cavity, fish were scanned from head to caudal region along the entire abdomen surface at a transverse plane. To maximize transmission, acoustic gel was applied to the probe surface. We used the ultrasound equipment (Aeroscan CD10 Pro/Plus) fitted with a high-density linear array probe with a frequency range of 7–17 MHz to scan each live fish's body cavity in the transverse plane, following the fundamental ultrasonography techniques [38]. The scan was carried out with a gain of 60–80% at a depth of 20–35 mm (Figure 3). The endpoints of the gonad were identified using ultrasonography, and the length was measured using a ruler from outside. Using ultrasonography, a transverse cross section of the gonad was digitally recorded at three evenly spaced locations along its length. Following ultrasonography, the fish was transferred quickly onto the dissection tray for gonad collection.

2.4. Gonadosomatic Index (GSI) and Fecundity Determination. After dissecting, the gonads were taken out of the body cavity, and the length and weight of the intact left and right lobes of ovary and testes were measured using a precision balance and vernier scale [39]. After measuring the gonad volume, gonad subsamples were stored in 10% neutral buffered formalin (NBF) for 24 h. GSI was calculated using the following formula: gonad weight/(body weight − gonad weight) × 100 [39]. Three aliquots from the anterior, middle, and posterior portions of both ovaries were removed and placed into Gilson's solution for 24–48 h to soften the connective tissues and harden the oocytes. Then, the aliquots of ovaries were removed from Gilson's solution, rinsed in water, and sieved through gauge cloths to remove disrupted tissues. Clumped eggs were dispersed by physical manipulation. The eggs were transferred to a small preweighed plastic sieve, excess water was removed by repeated blotting from outside, and total egg mass was weighed nearest to 0.01 g. Exact counts of each subsample were made under a dissecting microscope (Olympus, Japan). Absolute fecundity was measured by the gravimetric method [40] using the following formula: (no. of oocyte present in the ovarian subsample/weight of the ovarian subsample) × total weight of the ovary.

2.5. Estimation of Gonad Volume

2.5.1. Noninvasive USG-Based Shape Method. The gonad endpoint's images were accurately focused, and the length of each lobe was measured using a ruler. Transverse cross sections of the gonad were captured digitally at three different parts (anterior, middle, and posterior) to measure the diameters (R1, R2, and R3) digitally, and the volume of the gonad was estimated for each fish using the measurements obtained from the ultrasound images. A representative geometrical shape was constructed based on a visual examination of hilsa gonads [7]. The total gonad volume was estimated by summing the volumes of all geometric shapes formed by three cross-sectional diameters and external length measurement. The geometrical shape was based on a truncated cone and hemisphere. The overall shape was divided into four geometrical parts, and each part volume was calculated separately using the volume formula of individual shapes (Figure 4). Total USG estimated gonad volume = V1 + V2 + V3 + V4, Where, $V1 = 2/3\pi\ (R1)^3$, $V2 = 1/3\pi\ L1\ (R1^2 + R1 * R2 + R2^2)$, $V3 = 1/3\pi\ L2\ (R3^2 + R3 * R2 + R2^2)$, and $V4 = 2/3\pi\ (R3)^3$.

2.5.2. Invasive/True Method of Determining Gonad Volume. The volume of each dissected gonadal lobe of fish ($n = 15$ females and 15 males) was calculated using the water displacement method, which involved submerging the gonad lobe in a known volume of water and measuring the increase in volume. Total gonad volume was determined by adding the volume of left and right lobes.

2.5.3. Validation of GSI Measurements Using Shape and True Methods. To assess the effectiveness of ultrasonic imaging-based GSI determination, it was necessary to compare the GSI values obtained through the shape method with those determined by weighing the freshly dissected gonads. The volume of the gonad was estimated by establishing a linear correlation between the gonad volume measured through the shape and true methods. It is worth mentioning that the male and female hilsa used for ultrasonography had identical measurements to those intentionally sacrificed for this purpose.

2.6. Histological Examinations. Subsamples were removed from the anterior, middle, or posterior regions of the gonads and initially fixed in 10% NBF for 24 h. NBF was replaced by 70% ethanol for long-term storage. Fixed tissue samples were dehydrated in increasing series of different grades of ethanol [70, 80, 90, 95, and 100%] and then cleaned in xylene. Then, the tissue samples were infiltrated and embedded in paraffin with the help of a paraffin embedding station (Leica EG 1150H, Leica Microsystems, USA). Several 4 μm paraffin slices were cut with the help of a microtome (Leica RM2125RTS, Leica Microsystems, USA). The tissue sections were mounted on slides. Microscopic slides were kept in xylene for dewaxing and rehydrated through a series of graded ethanol (100, 95, 80, 70, and 50%). The sections

FIGURE 3: Ultrasonography of live riverine hilsa.

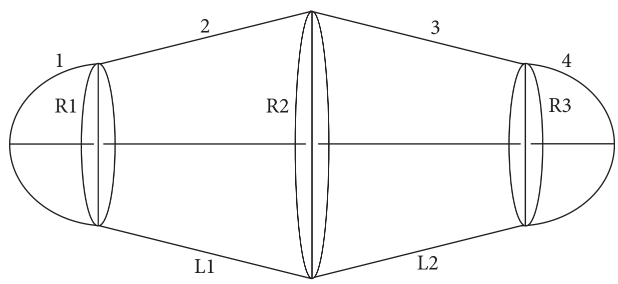

FIGURE 4: Use of a generic shape based on the external length measurements and ultrasound cross-sectional sections to estimate the hilsa gonad volume. Equations used to estimate the volume of each particular shape: for section 1 and 4, $V1 = 2/3\pi\,(R1)^3$ and $V4 = 2/3\pi\,(R3)^3$; for section 2 and 3, $V2 = 1/3\pi\ L1\ (R1^2 + R1 * R2 + R2^2)$ and $V3 = 1/3\pi\ L2\ (R3^2 + R3 * R2 + R2^2)$, where R is the radius and L is the length.

were then stained with hematoxylin (Harris, Himedia, India) and Eosin Yellow Stain solution (2% W/V, Nice, India). Again, dehydration was performed (50, 70, 80, 90, and 100% ethanol) following standard procedure and mounted with DPX [40]. Using an upright microscope (Leica DM 3000 LED, Leica Microsystems, USA), the slides were examined, and histomorphographs of various stages were captured on the Leica DFC 450 C camera. Ovaries were categorized based on the developmental stages of leading cohort oocytes following the methods described previously [39–41] with a slight modification. Leica Suite software was used to quantify the leading group of oocytes that were categorized based on the nucleus position, morphology, and distribution of yolk granules and oil globules [39]. Using the upright microscope (Leica DM 3000 LED), the maximum diameter of 50 mature oocytes was measured for each female ($n = 15$) from the preserved gonad samples. Three gonad samples were used to measure 50 oocytes of each stage with an accuracy of ±2%. Ray's histological criteria in *T. ilisha* were adhered to for staging males ($n = 15$) [39]. The presence or absence of spermatozoa within seminiferous tubules defined testicular stages based on the relative abundance of cysts containing the four types of spermatogenic cells, namely, spermatogonia, spermatocytes, spermatids, and spermatozoa.

2.7. Data Analysis. The GSIs from the USG images of ovary and testes were estimated using the "Shape method" and considered as calculated GSI. Data were expressed as mean ± standard error. Data were analyzed by one-way analysis of variance (ANOVA) followed by Duncan's multiple range test to determine the significant differences between the means using IBM-SPSS statistics version 20. All other correlations among length, weight, volume of gonads, and GSI were determined using simple linear regression. The degree of the relationship was measured based on the value obtained from the coefficient of determination (R^2). The b value was tested at a 95% confidence interval. The Pearson correlation coefficient (r) was used to assess the degree of correlation among the real gonad length, ultrasound-determined gonad length, real gonad volume, weight, USG-based gonad volume, and GSI.

3. Results

3.1. Sonographic Examination of Ovary and Testes. On an average, ultrasonographic scanning time per fish was about 1 to 2 min for identifying sex, but in the case of fish with immature gonads, it was hard to distinguish. The total time required to measure the gonad area precisely was 4 to 5 min. For the females belonging to different maturity stages, the early vitellogenic stage through the post-spawning stage, ultrasonographic measurement was done successfully for gonadal morphometrics. Ultrasound imaging of testes was done precisely in maturing males; imaging immature males' testes was often difficult due to their small size and similar appearance to adjacent organs, such as the kidney and liver (Figures 5 and 6). Although the USG-based sex identification of females carrying any size of the ovary was possible, the sex of the immature males could not be identified. The female hilsa gonads appeared light greyish on ultrasonography images during the early vitellogenic stage of maturity. At the post-spawning stage, the gonad appeared dark greyish in colour, and flaccidness of the ovary was also observed (Figure 5). The testes appeared dark in early spermatogenesis and late spermatogenesis, whereas they looked light grey in the early spermiating stage. During late spermiating and spent stages, it appeared dark greyish and visible clearly (Figure 6).

3.2. Calculation of the Gonad Volume through USG Imaging. A geometrical shape of the gonad was developed, and with the help of the shape method, the volume of different parts of the gonad was measured. In stage III or early vitellogenic stage in females, the mean USG gonad volumes for V1 and V4 were 0.385 and 0.204 cm^3, respectively, as these marginal portions had less density than the middle portion of the ovary as V2 and V3 indicating the volume as 11.202 and 9.024 cm^3, respectively (Table 1). For stage III, the total mean USG gonad volume was 20.816 cm^3, but as the stage advanced, the total mean USG gonad volume also increased. At late vitellogenic (stage IV) and final maturation (stage V) stages, mean total USG gonad volumes were 27.696 and 52.971 cm^3, respectively. But at the spawning (stage VI), the mean total USG gonad volume was 13.587 cm^3 which gradually decreased (Table 1). Similarly, for males, the mean total USG gonad volume differed at various maturity stages. In stages III (mature/early sperimating) and IV (spawning/late spermiating), total mean volume values were 2.281 and 4.019 cm^3, respectively, but in stage V (spent), the mean volume was 0.534 cm^3, which was the lowest among all (Table 2).

3.3. Gonad Length Determination. The real lengths of right and left ovary were highly correlated ($r = 0.99$) with that of the USG-determined lengths. The coefficient of determination (R^2) also described that >99.5% of the variation in USG-determined gonad's length accounted for the change of the real length of gonad in the linear relationships (Figures 7(a) and 7(b)). A similar high correlation ($r = 0.99$) and coefficient of determination ($R^2 > 0.99$) was observed between real and USG-based lengths of testes (Figures 7(c) and 7(d)).

3.4. Gonad Volume Determination. Gonad volume varied significantly ($P < 0.05$) with the progress of maturity in females and males (Figure 8). However, there was no significant difference ($P > 0.05$) between real and USG-based gonad volume at a particular maturity stage in both sexes (Figure 8). The correlation coefficient ($r \geq 0.98$) indicated a high correlation between real and USG-based gonad volume in females and males. The regression equation, $y = ax + b$, where y = USG gonad volume and x = real gonad volume, gave the values of intercept (b) and regression coefficient (a). The regression equations were calculated as $y = 0.9584x - 8.7152$, $R^2 = 0.9973$ for females (Figure 9(a)) and $y = 0.8519x - 0.5017$, $R^2 = 0.9656$ for males (Figure 9(b)). High correlation and coefficient of determination (R^2) between real and USG-based gonad volume indicated that the regression equations can determine the accurate volume based on the USG-based gonad volume in both sexes.

3.5. Gonad Volume and Gonad Weight Calculation. In females, real gonad weight was highly correlated with the real and USG gonad volume with a respective Pearson correlation coefficient value of 0.95 and 0.96. A high coefficient of determination ($R^2 > 91\%$) indicated that changes in ovary weight accounted for alteration in real as well as USG-based volume individually in the linear relationship of ovarian weight and volume measured differently (Figures 10(a) and 10(b)). Similarly, there were high correlation values ($r \geq 0.98$) and coefficient of determination ($R^2 \geq 0.97$) between the real testis weight and real/USG-based testis volume demonstrating a possibility of calculating accurate testes weight from the USG-based testes volume (Figures 10(c) and 10(d)).

3.6. GSI Calculation. The GSI calculated based on real gonad weight (real GSI) and USG-based gonad volume (calculated GSI) showed significant variation at different maturity stages in females and males (Tables 3 and 4). However, there were no significant differences between the real and calculated GSI values in females and males at a particular maturity stage (Tables 3 and 4). GSI values showed a strong correlation ($r = 0.77$) and a high coefficient of determination ($R^2 \geq 0.75$) with the real and USG-based volume of the ovary (Figures 11(a) and 11(b)). In males, there was a weak correlation ($r = \leq 0.48$) between GSI and testes volume based on real weight or USG-based volume, whereas a moderate correlation ($r = 0.51$ was noted between GSI and the real volume of testes (Table 5). Moreover, the coefficient of determination between 17% and 21% (Figures 11(c) and 11(d)) indicated that the volume of testes did not account for the changes in real and USG-based volumes.

3.7. Fecundity. From the sample analysis of 15 female fish, it was observed that the absolute fecundity of fish varied from 210548 to 1100542 eggs. The mean fecundity of 15 females was recorded as 543409 ± 260816 eggs with a mean total length of 331.36 ± 56.79 mm and mean body weight of 445.82 ± 190.27 g.

3.8. Histology. Microscopic observations of gonad histology demonstrated the change in cellular organization in the ovary during the progress of gonad maturation in females and males. In stage III, early vitellogenic oocytes (EV) were

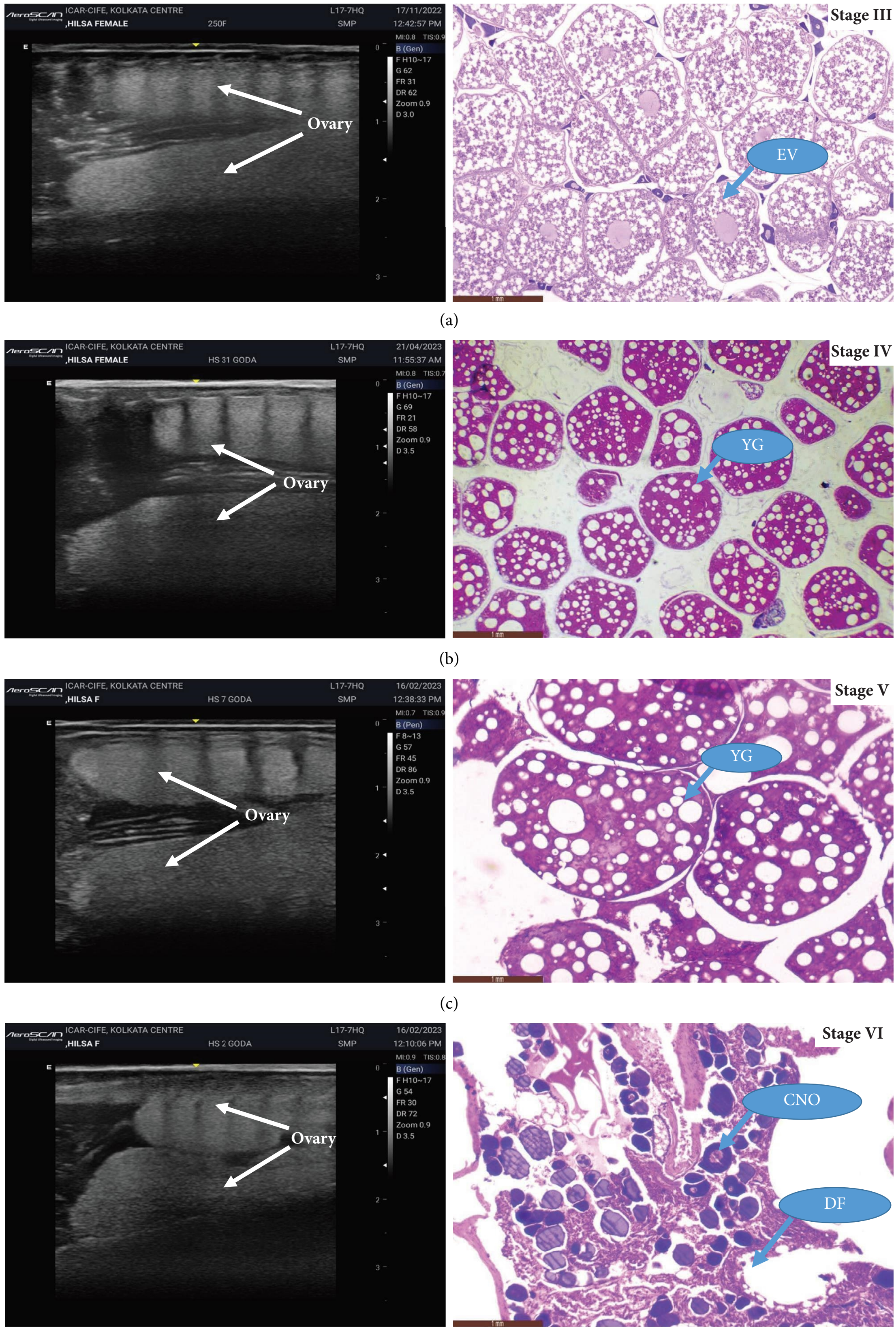

Figure 5: Ultrasonographic images of the female hilsa gonads at different stages. (a) Stage III (early vitellogenic), (b) stage IV (late vitellogenic), (c) stage V (final maturation), and (d) stage VI (spawning). Histology images of the female hilsa gonad at different maturity stages. (a) Stage III, (b) stage IV, (c) stage V, and (d) stage VI. EV: early vitellogenic, YG: yolk granules, CNO: chromatin nucleus, and DF: disintegrated follicles.

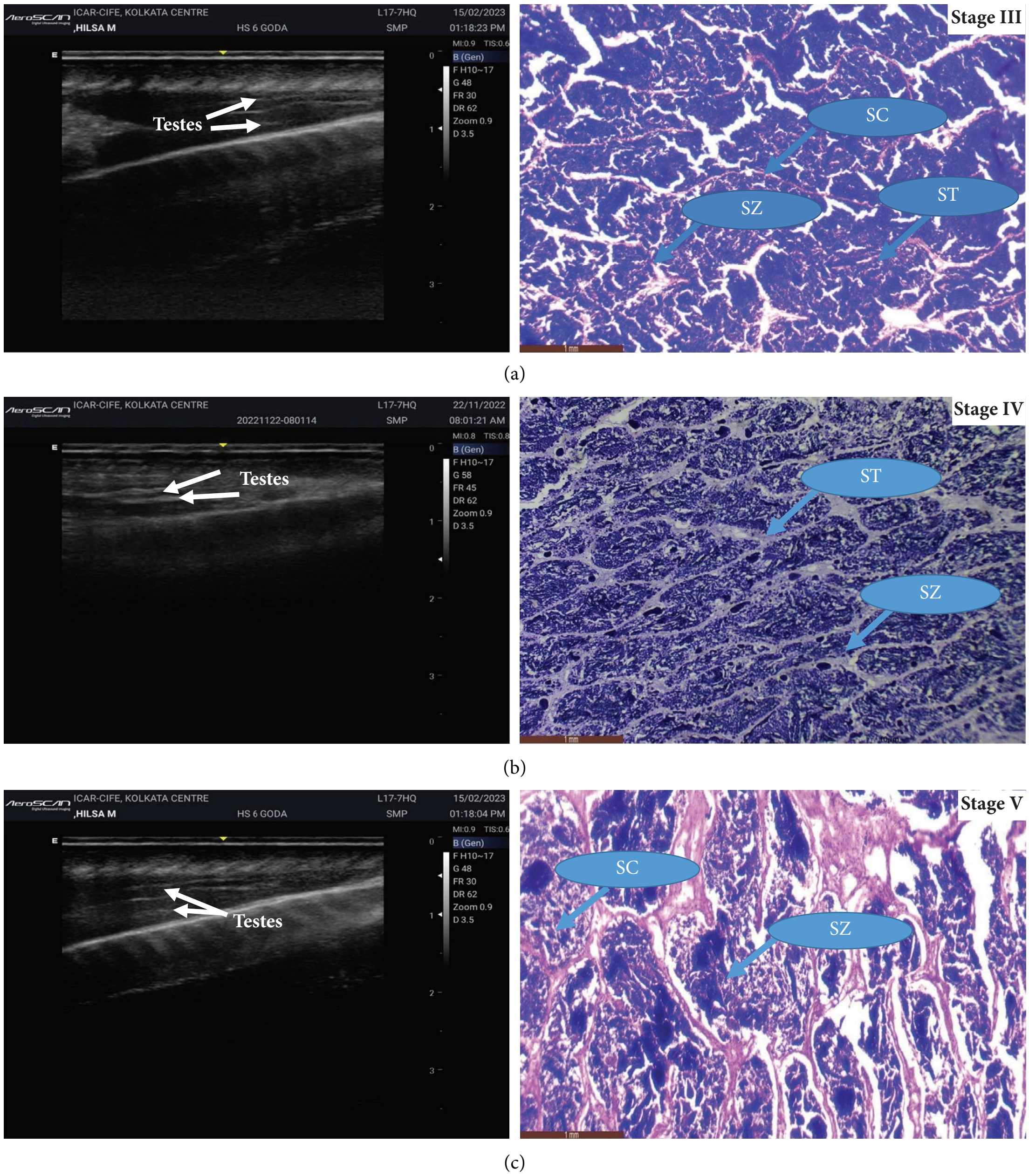

Figure 6: Ultrasonographic images of the male hilsa gonad at different stages. (a) Stage III (mature), (b) stage IV (spawning), and (c) stage V (spent). Histology images of the male hilsa gonad at different maturity stages. (a) Stage III, (b) stage IV, and (c) stage V. ST: spermatid, SZ: spermatozoa, and SC: spermatocyte.

Table 1: Volume (cm^3) calculation based on the shape method in female hilsa.

Sl. no.	Stage	V1	V2	V3	V4	Total
1	III	0.385	11.202	9.024	0.204	20.816
2	IV	0.673	13.758	12.813	0.4524	27.696
3	V	1.596	25.725	24.960	0.690	52.971
4	VI	0.214	7.021	6.321	0.031	13.587

Table 2: Volume (cm^3) calculation based on the shape method in male hilsa.

Sl. no.	Stage	V1	V2	V3	V4	Total
1	III	0.033	1.506	0.717	0.025	2.281
2	IV	0.082	2.525	1.375	0.037	4.019
3	V	0.005	0.325	0.201	0.003	0.534

observed (Figure 5(a)), while stage IV was characterized by the presence of vitellogenic oocytes (Figure 5(b)). Mature and ripe stages were characterized by a uniform distribution of yolk granule (YG) and oil globule (OG) in the cytoplasm, and the formation of yolk (Figures 5(c) and 5(d)). Similarly, changes in the testes were observed microscopically. In stage III (early spermiating), the spermatozoa number increased

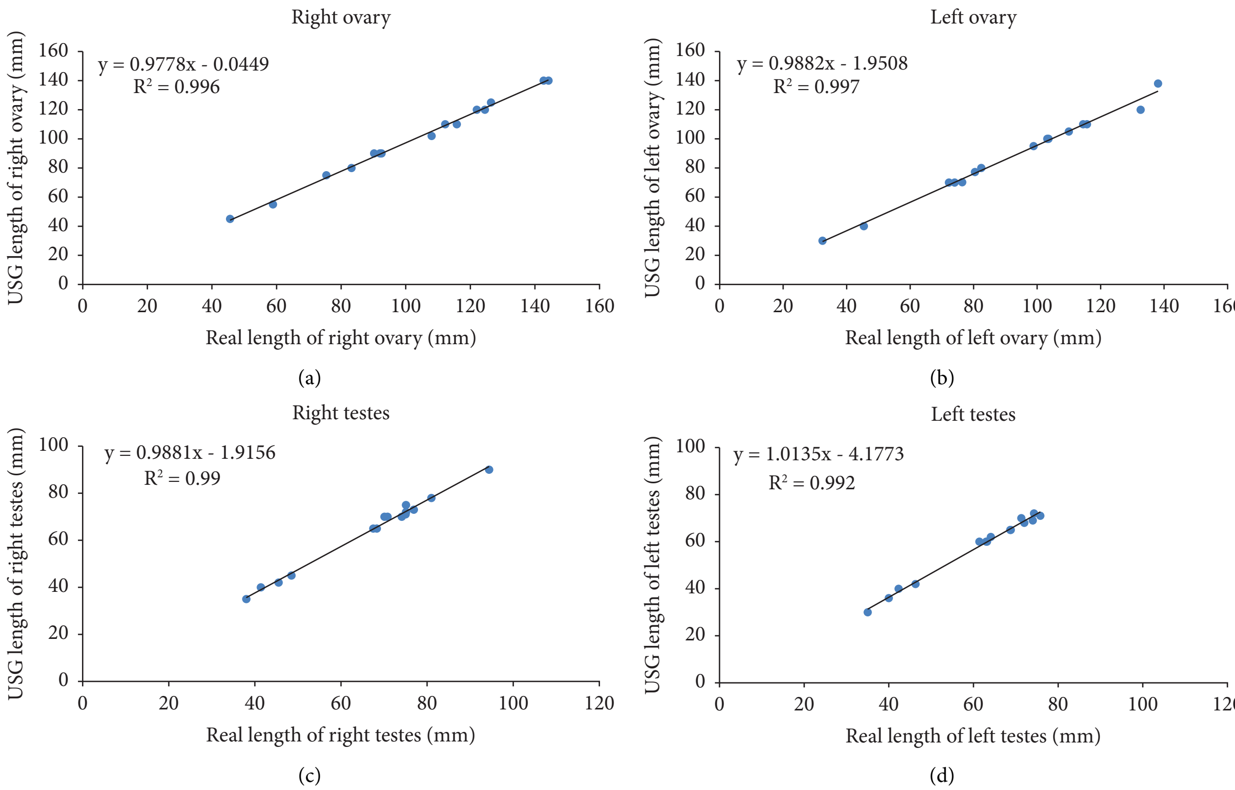

Figure 7: Linear relationship between USG-determined gonad length and real gonad length. (a) Female right ovary, (b) female left ovary, (c) male right testes, and (d) male left testes.

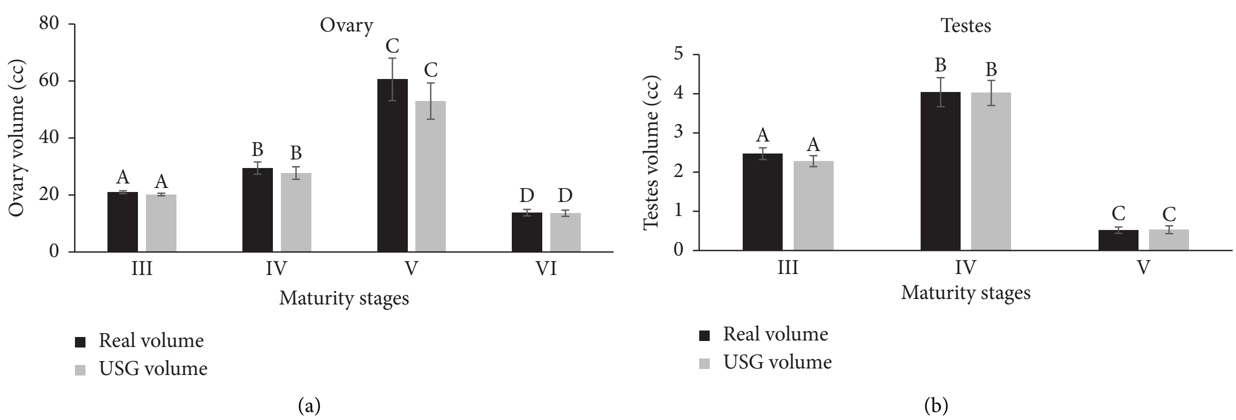

Figure 8: Ovary (a) and testes (b) volumes based on real volume and calculated on USG-based images of gonads. Different letters on bars denote significant differences between maturity stages at $P < 0.05$ level.

abruptly, and other spermatogenic cells were present adjacent to the tubular wall (Figure 6(a)). In stage IV, free spermatozoa occupied almost the entire tubules, while a narrow cluster of spermatocytes and spermatids was adjacent to the tubular wall. The tubules were elongated at this stage (Figure 6(b)). In stage V, the tubular wall was disrupted, and a few residual sperms, spermatocytes, and spermatogonia were present (Figure 6(c)).

4. Discussion

Previous studies reveal ultrasonography as the best noninvasive technique for determining sex and maturity in several fish species. The present study demonstrating a portable ultrasound machine which can be adapted for use on a boat, is a useful and reliable tool for identifying gender and gonad maturity assessment, especially for hilsa, which is

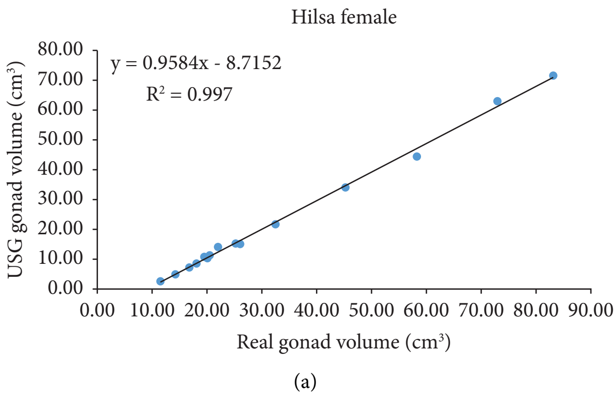

Figure 9: Linear relationship between USG-determined gonad volume and real gonad volume of hilsa. (a) Female and (b) male.

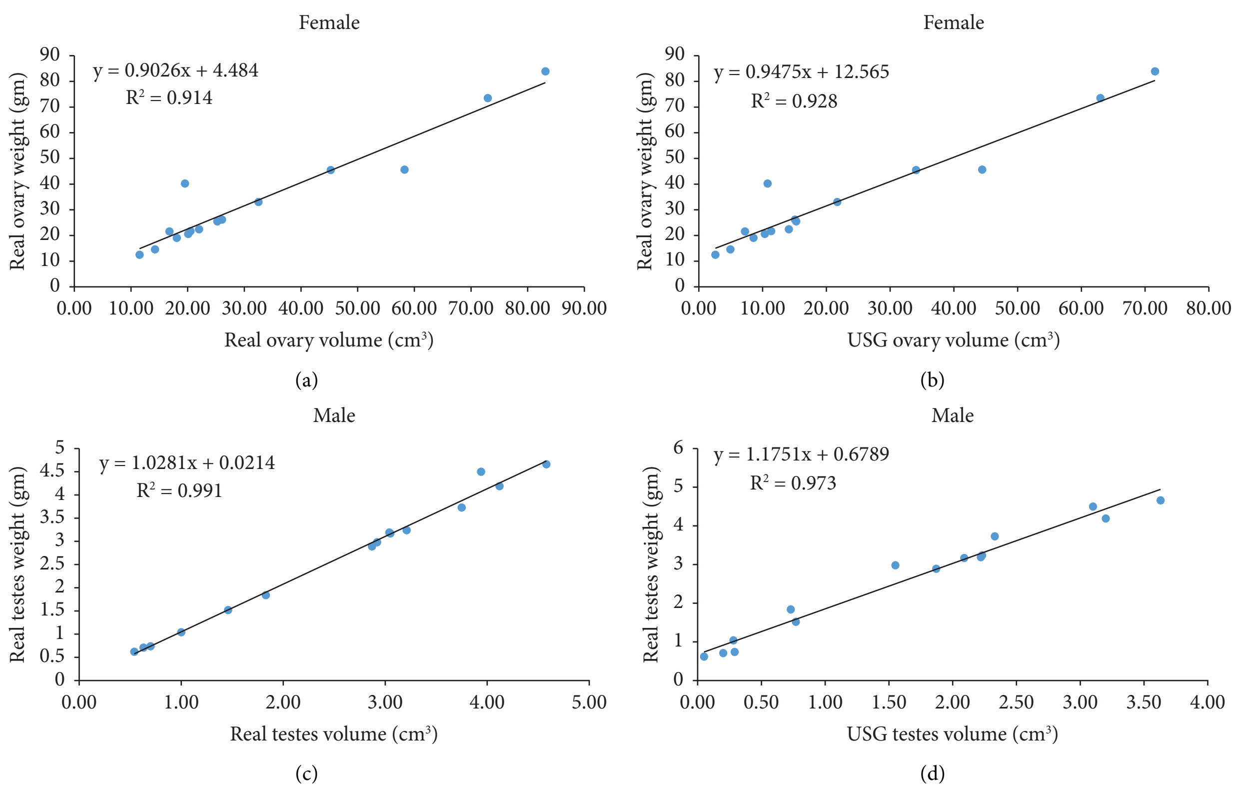

Figure 10: Comparative linear relationship between real gonad weight and real gonad volume with real gonad weight and USG-determined gonad volume of hilsa. (a) Real ovary weight vs. real ovary volume in females, (b) real ovary weight vs. USG-determined ovary volume in females, (c) real testes weight vs. real testes volume in males, and (d) real testes weight vs. USG-determined testes volume in males.

Table 3: Correlation between real GSI and calculated GSI in female hilsa.

Sl. no.	Stage	Real GSI	Calculated GSI	Correlation coefficient
1	III	10.44 ± 0.10	10.32 ± 0.02	0.965
2	IV	12.37 ± 0.89	11.79 ± 0.63	0.987
3	V	16.51 ± 1.15	15.57 ± 2.35	0.903
4	VI	4.66 ± 1.59	3.98 ± 1.11	0.949

highly expensive, stress-sensitive, and witnessing a decline in its fishery due to anthropogenic and climatic factors [42]. Before the ultrasonographic examination of *T. ilisha*, females were anesthetized to reduce handling stress. Then, body length and weight were measured, which ranged from 245 to 420 mm and 200 to 690 g, respectively. The male fish used for scanning ranged from 150 to 320 mm in length with body weight ranging from 250 to 320 g. In immature hilsa males

Table 4: Correlation between real GSI and calculated GSI in male hilsa.

Sl. no.	Stage	Real GSI	Calculated GSI	Correlation coefficient
1	III	1.27 ± 0.15	1.20 ± 0.18	0.864
2	IV	1.88 ± 0.27	1.75 ± 0.40	0.901
3	V	0.57 ± 0.16	0.49 ± 0.09	0.857

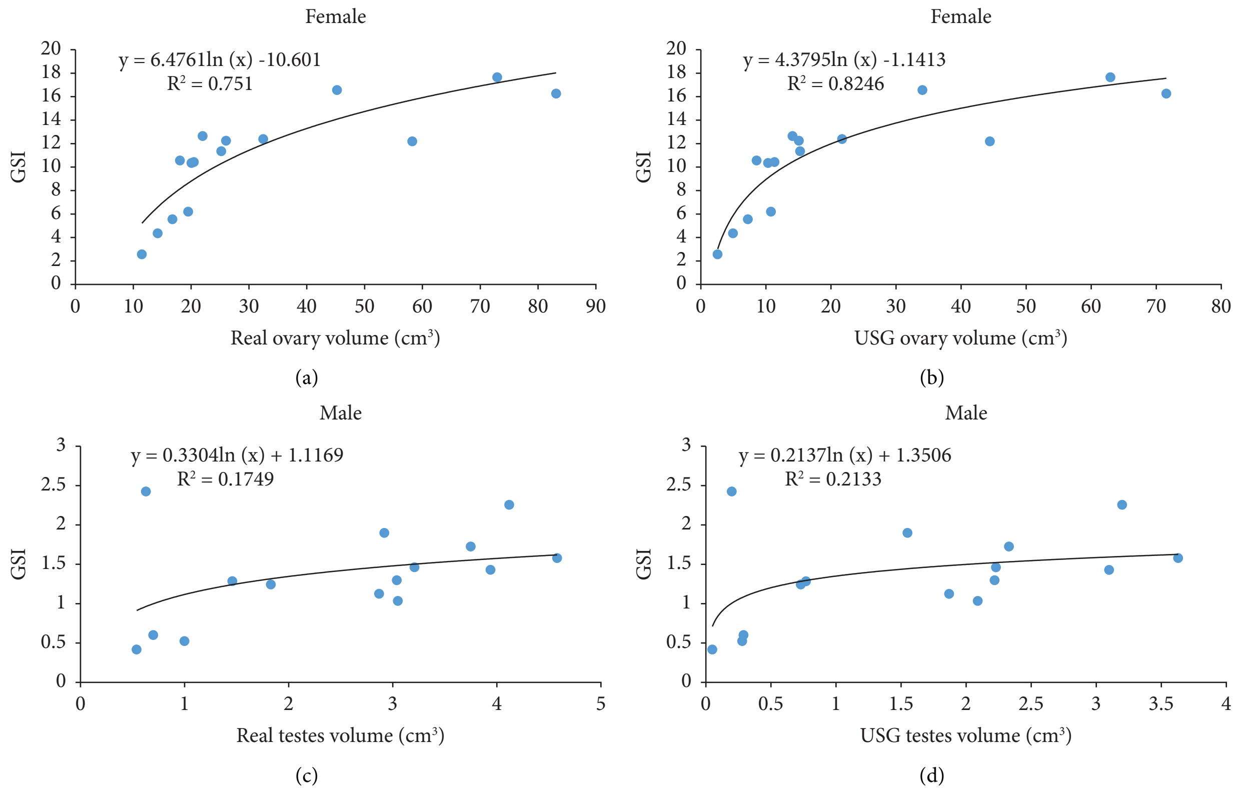

Figure 11: Comparative nonlinear relationship between real gonad volume and GSI with USG-determined gonad volume and GSI. (a) Real ovary volume vs. GSI in females, (b) USG-determined ovary volume vs. GSI in females, (c) real testes volume vs. GSI in males, and (d) USG-determined testes volume vs. GSI in males.

Table 5: Correlation among GSI values determined based on actual gonad weight, real gonad volume, and USG-based gonad volume in hilsa males.

	GW	GSIW	RGV	GSIRV	USV	GSIUSV
GW	1					
GSIW	0.44386	1				
RGV	**0.99574**	0.45446	1			
GSIRV	0.48836	**0.99238**	**0.50752**	1		
USV	**0.9866**	0.43818	**0.98266**	0.47831	1	
GSIUSV	0.44386	**1**	0.45446	**0.99238**	0.43818	1

Pearson correlation values (in bold), $r > 0.99$ indicated a positive strong correlation, whereas r values >0.50 denoted a moderate correlation. GW, actual gonad weight; GSIW, GSI based on GW; RGV, real gonad volume; GSIRV, GSI based on the RGV; USV, USG-based gonad volume; GSIUSV, GSI based on USV.

shorter than 250 mm in length and below 230 g body weight, gonads were not properly visible at scanning. Conversely, in the fish longer than 250 mm, gonads appeared visible in grey colour, organ ends were easy to detect, and contours were generally obvious on cross-sectional images.

Through ultrasonography, it was difficult to distinguish between immature (stage I and II) male and female hilsa below 250 mm in length. Since only riverine fish were used in this study, males and females of stages III and IV, which were present in rivers shortly before the spawning season, and V and VI, which were found almost throughout the spawning season, were sampled. The fish of stages, I and II were not available in sufficient quantity at the sampling locations during the study. Therefore, the fish of stages III, IV, V, and VI were the only subjects of this investigation. The female hilsa gonads appeared light greyish on ultrasonography during the early stages of maturity, while the male hilsa gonads seemed dark. In the early stages of the development in salmon, the gonads of females appeared light and granulated on ultrasonography, while the gonads of males looked dark and translucent [43]. While male gonads also became larger and had a lighter tone, female gonads mostly altered in size as they matured. Mature female gonadal ultrasound images displayed bright and granular structures with oocytes appearing as pale grey specks at the top of the screen. A distinct shadow was visible across from the transducer. Male mature gonads were shown to have coiled and twisted lobes and dark grey patches, or were "hypoechoic." Due to their small size, the gonads of juvenile males were hard to detect. In salmon, gonads are identified by exclusion, and a similar method was employed for sturgeons [44]. With the progress of maturity advancement, the female gonads became increasingly apparent under ultrasonography. Mature male gonads resembled a structure that was light grey. In an earlier study, the gender and maturity of juvenile and adult halibut (*Hippoglossus hippoglossus*), mature winter flounder (*Pleuronectes americanus*), yellowtail flounder (*Pleuronectes ferruginea*), and mature haddock (*Melanogrammus aeglefinus*) were identified employing ultrasonography imaging [28]. Mature and immature ovaries could be readily distinguished in females, whereas only mature testes were reliably distinguished in males. Ultrasound can also be used to evaluate the ovulatory cycles of halibut and the ovarian maturation of haddock. The potential of ultrasonography to ascertain *T. ilisha* sex, gonad size, and maturity has been successfully demonstrated in the current study.

In this study, the shape method was used to determine the volume of different parts of the gonad of both male and female hilsa. It was observed that the gonad volume increased with the GSI increase, simultaneously with the advances in maturity stages and subsequent increase in gonad weight. Here, two shapes were used; one was a truncated cone and another was a hemisphere. In the pallid sturgeon [7], they used a hemisphere, truncated cone, and cylinder, while according to Lagler et al. [45], a generic shape using a cone and the truncated cone was designed based on the gonad structure. Both in pallid sturgeon and eel, this shape method was effective as a noninvasive and nonlethal tool for gonad volume measurement. However, as the mass of eel gonad increased, this shape method became more underestimated, but Lagler et al. [45] found five cross sections as the best method to predict gonad volume. In this study, gonad length and diameter were measured using ultrasonography and used in the shape technique, whereas in cases of eel and sturgeon, area and length were used to calculate the radius. Using ultrasonography, two methods were attempted for estimating the mass of ovaries in silver eels: one based on a linear model and another on calculating the ovary volume from a representation of gonad morphology [36]. Ultrasonography achieved 100% success in determining the sex of male and female hilsa. The present study revealed, for the first time, that the ultrasound could accurately measure gonad volume using the shape method, except for immature stages I and II for male and female hilsa.

We also established that ultrasonography could measure the gonad length externally with high accuracy (Figure 7) avoiding the potential effects of injuring gonads and muscles without causing handling stress to the fish. We found that the average ultrasonic gonad volumes were not significantly less than the real volumes, which does not corroborate with the earlier report in shovelnose sturgeon. The USG gonad volume was less (>4.92 cm^3) than the real gonad volume in shovelnose sturgeon [7]. Gonad volume significantly changes in hilsa within the gender, maturity stages, and month. As fish become mature, the volume of gonad increases along with its weight. In this study, we found no difference between USG estimated and real gonad volumes. The actual ovarian mass and the estimated ovarian mass from ultrasonography had a significant correlation ($R^2 = 0.97$) in silver eels [36]. In our study, real and calculated gonad volumes were not different, highly correlated, and showed a high coefficient of determination (R^2). Thus, we could calculate the real gonad volume from the USG gonad volume using the regression equation. Real gonad volume was correlated with real gonad weight and USG measured gonad volume and vice-versa in this study (Figure 7).

GSI is the percentage of gonad weight and body weight ratio. It was observed that body weight did not have any relation with gonad weight in the case of hilsa. Sometimes, this fish becomes mature early without attaining the required body weight, so there was a variation in volume and GSI [39]. Therefore, GSI could not be calculated accurately using gonad volume, particularly in males due to the low volume of the testes associated with wide variation in body weight. Nevertheless, from USG volume, we could easily calculate the real weight of gonad, to determine the accurate GSI, and from the calculated GSI, the maturity stages can be assessed using the GSI scale of maturity stages [39]. After identifying the microscopic maturity stage, the calculated GSI was matched to the corresponding maturity stage to validate the USG-based calculation of gonad volume to determine accurate stages. The study showed no difference among the stage-specific actual, real, and calculated GSI in males and females.

Fish have a wide range of fecundity [46], and the quantity of eggs produced by a female depends on various characteristics, including size, age, condition, and species [45]. Based on several breeding experiments, it was concluded that a species' ability to reproduce depends on a variety of factors, including food and space availability [46]. It was observed that smaller fish (total length: 253 mm and body weight: 200 g) carried 210,548 eggs, while the larger specimen (total length: 430 mm and body weight: 850 g) contained 10,71262 eggs. However, fish of similar length varied in their fertility. A fish with a total length of 380 mm and a body weight of 653 g had 8,48,042 eggs, while another fish with the same total length contained 7,20,256 eggs. The same species had similar fecundity variation in Bangladesh as well [47]. Further, the same kind of variation was also documented in this species [48, 49]. This study revealed that the average diameter of ova varied between 206.58 and 780.25 μm. In a previous study, similar results were reported [39, 40] stating that the ova diameter ranged from 728 to 850 μm at the mature stage. In contrast, the average oocyte diameter was reported to be between 475 and 564 μm during the maturity stage V and between 53 and 321 μm during stage VI (spawning) [39].

The present study categorized the maturity stages of hilsa into six to seven stages for females, based on the observations by different authors with slight modifications [39–41, 49–51]. The classification of maturity status was as follows: I for immature, II for early growth, III for mid-growth, IV for final maturation, V for spawning capable, and VI for active spawning in females. The stage II gonad is known as the "oil droplets" stage, as "cortical alveolar vesicles" are present rarely in the oocytes, similar to many other fishes [52]. For males, the maturity stages were classified as I for immature, II for developing, III for mature, IV for spawning, and V for post-spawning based on García-López et al. [53], with a slight modification. In *T. ilisha*, the nucleus occupied the major portion of ooplasm in the chromatin nucleolus stage. Basophilic cytoplasm was produced by free ribosome accumulation [54]. Nucleoli of various sizes grouped around the inner lining of nucleus as the oocytes transformed to the perinucleolar stage as reported in the chromatin nucleolus stage in *Dicentrarchus labrax*. Each nucleolus in *Danio rerio* broke into multiple smaller nucleoli [55]. The synthesis process in the nucleus is responsible for changes in the nucleus and nucleolus during the phases of oocyte growth. At the commencement of the spawning season, the cortical alveolus serves as a marker of oocyte maturation [39]. The cortical alveoli and follicular layer encircling the oocytes are the most notable characteristics of a stage. There have been reports of three different forms of yolk in teleost oocytes: lipid droplets, yolk vesicles (cortical alveoli), and yolk granules [52]. The intracellular vacuolization in oocytes in many teleosts starts on the periphery and moves into the core of the oocyte [56]. Alveoli occur simultaneously surrounding the oocyte in the Japanese eel [57]. The oocyte attained its maximum size during post-vitellogenesis. The increase in oocyte size was attributed to the accumulation of exogenous yolk protein precursors; however, the accumulation of endogenous ones has also been recorded in several species [56]. The mature oocyte of *T. ilisha* was observed to have heterogeneous yolk vacuoles. As vitellogenesis comes to an end, the nucleus begins to migrate toward the animal pole as a result of yolk vesicle buildup in the cytoplasm of cells. *T. ilisha* has been regarded as a group synchronous and total spawner [39], as a dominant stage of oocytes was observed at each sampling time along with very few of the other stages. Similar conditions for *Acanthopagrus latu*s in the Persian Gulf were also described [58]. The study demonstrated an accurate assessment of the maturity stages of hilsa based on ultrasonic images and GSIs calculated from USG gonad volume [59]. Thus, the study confirms that the actual maturity stages can be easily assessed based on ultrasound images of the gonads of mature hilsa.

5. Conclusion

Using a basic ultrasound procedure, the determination of sex and maturity stages was standardized in mature hilsa of both sexes avoiding injuries and handling stress, preventing progress of normal gonad development. The real gonad volume of fish was measured and compared with the calculated volume based on the USG image to develop a linear equation to estimate real or actual volume from the USG gonad volume. The accurate GSI and maturity stages were assessed easily from the USG gonad volume. Further, supporting histological slides of different maturity stages were combined with the respective fish's ultrasonic image of the gonad to validate the calculated GSI to predict the respective maturity stage of both male and female hilsa. Therefore, this reliable, noninvasive technique of assessing gender and maturity stages in hilsa will contribute to gaining insight into the reproductive cycle of captive and wild hilsa to develop brood management practices aiming at artificial reproduction and eventually conservation of the priced hilsa fishery.

Data Availability

Data are included within the article.

Disclosure

The preliminary data of the study were presented in the conference, 13th Indian Fisheries and Aquaculture Forum, February 23–25, 2024, Kolkata, India.

Conflicts of Interest

The authors declare that they have no conflicts of interest.

Authors' Contributions

SD and GB conceptualized and supervised the study, performed project administration and funding acquisition; GT, MAP, and TKG reviewed and edited the study; PKS, TJ, and PM performed the experiment and prepared the original draft; SK, DD, and SA visualized the study; RKM and AKS performed data analysis.

Acknowledgments

This research was supported by the National Agricultural Science Fund (NASF), Indian Council of Agricultural Research, New Delhi, India, under the project entitled, "Captive Breeding of Hilsa, *Tenualosa ilisha*: Phase II" (NASF/ABA(SM)-8026/2020-21). The authors are grateful to the Director/Vice-Chancellor, ICAR-Central Institute of Fisheries Education, Mumbai, for providing facilities to conduct the research work.

References

[1] J. D. Tan-Fermin, S. Ijiri, H. Ueda, S. Adachi, and K. Yamauchi, "Ovarian development and serum steroid hormone profiles in hatchery-bred female catfish *Clarias macrocephalus* (Gunther) during an annual reproductive cycle," *Fisheries Science*, vol. 63, no. 6, pp. 867–872, 1997.

[2] A. Manosroi, K. Meng-umphan, and J. Manosroi, "Annual sex hormonal profiles, gonad development and age determination

of the Mekong giant catfish (*Pangasianodon gigas*, Chevey)," *Aquaculture Research*, vol. 34, no. 15, pp. 1379–1385, 2003.

[3] A. Golpour, M. Pšenička, and H. Niksirat, "Ultrastructural localization of intracellular calcium during spermatogenesis of sterlet (*Acipenser ruthenus*)," *Microscopy and Microanalysis*, vol. 22, no. 6, pp. 1155–1161, 2016.

[4] A. Golpour, M. Pšenička, and H. Niksirat, "Subcellular distribution of calcium during spermatogenesis of zebrafish, *Danio rerio*," *Journal of Morphology*, vol. 278, no. 8, pp. 1149–1159, 2017.

[5] A. Golpour, C. Broquard, S. Milla et al., "Determination of annual reproductive cycle in male sterlet, *Acipenser ruthenus* using histology and ultrasound imaging," *Fish Physiology and Biochemistry*, vol. 47, no. 3, pp. 703–711, 2021.

[6] M. L. Wildhaber, D. M. Papoulias, A. J. DeLonay et al., "Gender identification of shovelnose sturgeon using ultrasonic and endoscopic imagery and the application of the method to the pallid sturgeon," *Journal of Fish Biology*, vol. 67, no. 1, pp. 114–132, 2005.

[7] B. J. Bryan, M. L. Wildhaber, D. M. Papoulias, A. J. DeLonay, D. E. Tillitt, and M. L. Annis, "Estimation of gonad volume, fecundity, and reproductive stage of shovelnose sturgeon using sonography and endoscopy with application to the endangered pallid sturgeon," *Journal of Applied Ichthyology*, vol. 23, no. 4, pp. 411–419, 2007.

[8] A. Hurvitz, K. Jackson, G. Degani, and B. Levavi-Sivan, "Use of endoscopy for gender and ovarian stage determinations in Russian sturgeon (*Acipenser gueldenstaedtii*) grown in aquaculture," *Aquaculture*, vol. 270, no. 1-4, pp. 158–166, 2007.

[9] M. S. Chebanov and E. V. Galich, "Ultrasound diagnostics for sturgeon broodstock management," 6th International Symposium on Sturgeon, p. 47, 2009.

[10] S. J. Divers, S. S. Boone, J. J. Hoover et al., "Field endoscopy for identifying gender, reproductive stage and gonadal anomalies in free-ranging sturgeon (*Scaphirhynchus*) from the lower Mississippi River," *Journal of Applied Ichthyology*, vol. 25, pp. 68–74, 2009.

[11] A. K. Sahoo, M. A. Wahab, M. Phillips et al., "Breeding and culture status of hilsa (*Tenualosa ilisha*, ham. 1822) in South Asia: a review," *Reviews in Aquaculture*, vol. 10, no. 1, pp. 96–110, 2018.

[12] M. S. Hossain, S. M. Sharifuzzaman, M. A. Rouf et al., "Tropical hilsa shad (*Tenualosa ilisha*): biology, fishery and management," *Fish and Fisheries*, vol. 20, no. 1, pp. 44–65, 2018.

[13] M. A. Khan, M. A. Wahab, A. M. Haque, M. Nahiduzzaman, and M. J. Phillips, "Value chain impact of the increased hilsa shad (*Tenualosa ilisha*) harvest in Bangladesh," *The International Food and Agribusiness Management Review*, vol. 23, no. 3, pp. 355–368, 2020.

[14] I. Porras, E. Y. Mohammed, L. Ali, M. S. Ali, and M. B. Hossain, "Power, profits and payments for ecosystem services in *Hilsa* fisheries in Bangladesh: a value chain analysis," *Marine Policy*, vol. 84, pp. 60–68, 2017.

[15] D. A. Milton, "Status of hilsa (*Tenualosa ilisha*) management in the Bay of Bengal," *BOBLME 2010 Ecology 01*, 2010.

[16] M. J. Rahman, M. A. Wahab, M. Nahiduzzaman, A. B. M. M. Haque, and P. Cohen, "Hilsa fishery management in Bangladesh," *IOP Conference Series: Earth and Environmental Science*, vol. 414, no. 1, p. 012018, Article ID 012018, 2020.

[17] R. Froese and D. Pauly, "FishBase, world wide web electronic publication," 2016, https://www.fishbase.org.

[18] S. Mackinson, U. R. Sumaila, and T. J. Pitcher, "Bioeconomics and catchability: fish and fishers' behaviour during stock collapse," *Fisheries Research*, vol. 31, no. 1-2, pp. 11–17, 1997.

[19] A. K. M. N. Alam, B. P. Mohanty, E. M. Hoq, and S. Thilshed, "Nutritional values, consumption and utilization of Hilsa *Tenualosa ilisha* (Hamilton 1822)," in *Proceedings of Regional Workshop on Hilsa: Potential for Aquaculture*, Dhaka, Bangladesh, September 2012.

[20] S. Dutta, K. Chakraborty, and S. Hazra, "Life history and population dynamics of *Tenualosa ilisha* of Sundarban Estuary in Bay of Bengal, India for sustainable fishery management," *Indian Journal of Geo-Marine Science*, vol. 48, no. 12, pp. 1870–1880, 2019.

[21] M. M. Islam, E. Y. Mohammed, and L. Ali, "Economic incentives for sustainable hilsa fishing in Bangladesh: an analysis of the legal and institutional framework," *Marine Policy*, vol. 68, pp. 8–22, 2016.

[22] GOWB, *The Gazette Notifications of Amendments on Hilsa Fishery*, Fisheries Department, Government of West Bengal, Kolkata, India, 2013.

[23] BOBLME, Management Advisory for the Bay of Bengal Hilsa Fishery, Regional Fisheries Management Advisory Committee, 2012.

[24] D. N. Chattopadhyaya, A. Chakraborty, P. K. Roy et al., "Protocols of Artificial breeding, egg incubation, spawn production and seed rearing of Hilsa shad (*Tenualosa ilisha*)—a high-value food fish," *ICAR-CIFA Extension Series No*, vol. 60, pp. 1–44, 2020.

[25] E. Reimers, P. Landmark, T. Sorsdal, E. Bohmer, and T. Solum, pp. 41–44, 1987, Determination of salmonids' sex, maturation and size: an ultrasound and photocell approach.

[26] E. Reimers, A. G. Kjørrefjord, and S. M. Stavøstrand, "Compensatory growth and reduced maturation in second sea winter farmed Atlantic salmon following starvation in February and March," *Journal of Fish Biology*, vol. 43, no. 5, pp. 805–810, 1993.

[27] S. A. Bonar, G. L. Thomas, G. B. Pauley, and R. W. Martin, "Management briefs: use of ultrasonic images for rapid nonlethal determination of sex and maturity of Pacific herring," *North American Journal of Fisheries Management*, vol. 9, no. 3, pp. 364–366, 1989.

[28] D. J. Martin-Robichaud and M. Rommens, "Assessment of sex and evaluation of ovarian maturation of fish using ultrasonography," *Aquaculture Research*, vol. 32, no. 2, pp. 113–120, 2001.

[29] C. A. Jennings, T. A. Will, and T. R. Reinert, "Efficacy of a high-and low-frequency ultrasonic probe for measuring ovary volume and estimating fecundity of striped bass *Morone saxatilis* in the Savannah River Estuary," *Fisheries Research*, vol. 76, no. 3, pp. 445–453, 2005.

[30] F. J. McEvoy, J. Tomkiewicz, J. G. Støttrup, J. L. Overton, C. McEvoy, and E. Svalastoga, "Determination of fish gender using fractal analysis of ultrasound images," *Veterinary Radiology and Ultrasound*, vol. 50, no. 5, pp. 519–524, 2009.

[31] J. M. Whittamore, C. Bloomer, G. M. Hanna, and I. D. McCarthy, "Evaluating ultrasonography as a non-lethal method for the assessment of maturity in oviparous elasmobranchs," *Marine Biology*, vol. 157, no. 12, pp. 2613–2624, 2010.

[32] M. Masoudifard, A. R. Vajhi, M. Moghim, R. M. Nazari, A. R. Naghavi, and M. Sohrabnejad, "High validity sex determination of three years old cultured beluga sturgeon (*Huso huso*) using ultrasonography," *Journal of Applied Ichthyology*, vol. 27, no. 2, pp. 643–647, 2011.

[33] B. T. Petochi, P. Di Marco, V. Donadelli et al., "Sex and reproductive stage identification of sturgeon hybrids (*Acipenser naccarii* × *Acipenser baerii*) using different tools: ultrasounds, histology and sex steroids," *Journal of Applied Ichthyology*, vol. 27, no. 2, pp. 637–642, 2011.
[34] A. M. Guitreau, B. E. Eilts, N. D. Novelo, and T. R. Tiersch, "Fish handling and ultrasound procedures for viewing the ovary of submersed, non-anesthetized, unrestrained Channel catfish," *North American Journal of Aquaculture*, vol. 74, no. 2, pp. 182–187, 2012.
[35] P. Hliwa, M. Bah, H. Kuźmiński, S. Dobosz, and A. Ciereszko, "Ultrasound evaluation of the gonadal structure in sex-reversed rainbow trout females," *Aquaculture International*, vol. 22, no. 1, pp. 89–96, 2014.
[36] S. Bureau du Colombier, L. Jacobs, C. Gesset, P. Elie, and P. Lambert, "Ultrasonography as a non-invasive tool for sex determination and maturation monitoring in silver eels," *Fisheries Research*, vol. 164, pp. 50–58, 2015.
[37] X. Leng, H. Du, W. Xiong, P. Cheng, J. Luo, and J. Wu, "Successful ultrasonography-assisted artificial reproduction of critically endangered Sichuan taimen (*Hucho bleekeri*)," *Fishes*, vol. 8, no. 3, p. 152, 2023.
[38] W. Zweibel and R. Sohaey, *Basic Ultrasound Physics and Instrumentation", Introduction to Ultrasound*, WB Saunders, Philadelphia, PA, USA, 1998.
[39] S. K. Ray, S. Dutta, G. H. Pailan, V. R. Suresh, and S. Dasgupta, "Hormonal signatures of gonad maturity and seasonality of spawning in migrating hilsa, *Tenualosa ilisha*," *Environmental Biology of Fishes*, vol. 105, no. 1, pp. 37–53, 2022.
[40] P. Kumar, N. K. Chandan, G. Biswas et al., "Fatty acid mobilization and histological changes at different maturation stages of female hilsa, *Tenualosa ilisha*," *Aquaculture*, vol. 576, Article ID 739887, 2023.
[41] K. Coward and N. R. Bromage, "Histological classification of oocyte growth and the dynamics of ovarian recrudescence in *Tilapia zillii*," *Journal of Fish Biology*, vol. 53, no. 2, pp. 285–302, 1998.
[42] T. Bandara and L. Wijewardene, "Global research effort on hilsa shad (*Tenualosa ilisha*)- insights from scientometrics," *Thalassas*, vol. 39, no. 2, pp. 981–996, 2023.
[43] N. S. Mattson, "A new method to determine sex and gonad size in live fishes by using ultrasonography," *Journal of Fish Biology*, vol. 39, no. 5, pp. 673–677, 1991.
[44] M. Moghim, A. R. Vajhi, A. Veshkini, and M. Masoudifard, "Determination of sex and maturity in *Acipenser stellatus* by using ultrasonography," *Journal of Applied Ichthyology*, vol. 18, no. 4-6, pp. 325–328, 2002.
[45] K. F. Lagler, J. F. Z. Bardach, and R. R. Miller, *Ichthyology*, John Wiley and Sons, Inc, New York, NY, USA, 1967.
[46] S. Doha and M. A. Hye, "Fecundity of Padma river hilsa (*H. ilisha*)," *Pakistan Journal of Science*, vol. 22, pp. 176–184, 1970.
[47] M. A. Akter, M. D. Hossain, M. K. Hossain, R. Afza, and A. S. Bhuyian, "The fecundity of *Hilsa ilisha* from the river Padma near Godagari of Rajshahi district," *University Journal of Zoology, Rajshahi University*, vol. 26, pp. 41–44, 1970.
[48] F. Hamilton, in *An account of the fishes found in the river Ganges and its branches*, 1822.
[49] S. L. Hora, "A preliminary note on the spawning grounds and bionomics of the so-called Indian Shad, *Hilsa ilisha* (Ham.) in the river Ganges," *Records of the Zoological Survey of India*, vol. 40, no. 2, pp. 147–158, 1938.
[50] R. H. Bucholtz, J. Tomkiewicz, and J. Dalskov, "Manual to determine gonadal maturity of herring (*Clupea harengus* L.)," in *DTU Aqua Report 197-08*, National Institute of Aquatic Resources, Charlottenlund, Denmark, 2008.
[51] P. J. Wright, "Understanding the maturation process for field investigations of fisheries-induced evolution," *Marine Ecology Progress Series*, vol. 335, pp. 279–283, 2007.
[52] H. J. Grier, M. C. Uribe, and R. R. Pattino, "The ovary, folliculogenesis, and oogenesis in teleosts," *Journal of Fish Biology*, vol. 43, pp. 25–84, 2009.
[53] Á. García-López, V. Fernández-Pasquier, E. Couto, A. V. Canario, C. Sarasquete, and G. Martínez-Rodríguez, "Testicular development and plasma sex steroid levels in cultured male Senegalese sole *Solea senegalensis* Kaup," *General and Comparative Endocrinology*, vol. 147, no. 3, pp. 343–351, 2006.
[54] M. Bariche, M. Torres, and E. Azzurro, "The presence of the invasive lionfish (*Pterois miles*) in the Mediterranean Sea," *Mediterranean Marine Science*, vol. 14, no. 2, pp. 292–294, 2013.
[55] O. Cakici and S. Ucuncu, "Oocyte development in the zebrafish, *Danio rerio* (Teleostei: cyprinidae)," *Journal of Fisheries and Aquatic Sciences*, vol. 24, pp. 137–141, 2007.
[56] R. A. Wallace and K. Selman, "Cellular and dynamic aspects of oocyte growth in teleosts," *American Zoologist*, vol. 21, no. 2, pp. 325–343, 1981.
[57] T. Kayaba, N. Takeda, S. Adachi, and K. Yamauchi, "Ultrastructure of the oocytes of the Japanese eel *Anguilla japonica* during artificially induced sexual maturation," *Fisheries Science*, vol. 67, no. 5, pp. 870–879, 2001.
[58] S. H. Karimi, P. Kochinian, and A. P. Salati, "The effect of sexuality on some haematological parameters of the yellowfin seabream, *Acanthopagrus latus* in the Persian Gulf," *Iranian Journal of Veterinary Research*, vol. 14, pp. 65–68, 2013.
[59] S. Dasgupta, G. Biswas, G. Tripathi et al., "Determination of sex, gonad volume and maturity status of the Indian shad, *Tenualosa ilisha* using ultrasonography: a rapid and non-lethal tool," in *Book of Abstracts, 13th Indian Fisheries and Aquaculture Forum*, p. 109, ICAR-Central Inland Fisheries Research Institute, Kolkata, India, 2024.